

Study of (n,2n) reaction on $^{191,193}\text{Ir}$ isotopes and isomeric cross section ratios

R. Vlastou^{1,a}, A. Kalamara¹, M. Kokkoris¹, N. Patronis³, M. Serris², M. Georgoulakis¹, S. Hassapoglou¹, K. Kobothisanis¹, M. Axiotis⁴, and A. Lagoyannis⁴

¹ Department of Physics, National Technical University of Athens, Athens, Greece

² Hellenic Army Academy, Athens, Greece

³ Department of Physics, University of Ioannina, Ioannina, Greece

⁴ Institute of Nuclear and Particle Physics, NCSR “Demokritos”, Athens, Greece

Abstract. The cross section of $^{191}\text{Ir}(n,2n)^{190}\text{Ir}^{g+m1}$ and $^{191}\text{Ir}(n,2n)^{190}\text{Ir}^{m2}$ reactions has been measured at 17.1 and 20.9 MeV neutron energies at the 5.5 MV tandem T11/25 Accelerator Laboratory of NCSR “Demokritos”, using the activation method. The neutron beams were produced by means of the $^3\text{H}(d,n)^4\text{He}$ reaction at a flux of the order of $2 \times 10^5 \text{ n/cm}^2\text{s}$. The neutron flux has been deduced implementing the $^{27}\text{Al}(n,\alpha)$ reaction, while the flux variation of the neutron beam was monitored by using a BF₃ detector. The $^{193}\text{Ir}(n,2n)^{192}\text{Ir}$ reaction cross section has also been determined, taking into account the contribution from the contaminant $^{191}\text{Ir}(n,\gamma)^{192}\text{Ir}$ reaction. The correction method is based on the existing data in ENDF for the contaminant reaction, convoluted with the neutron spectra which have been extensively studied by means of simulations using the NeusDesc and MCNP codes. Statistical model calculations using the code EMPIRE 3.2.2 and taking into account pre-equilibrium emission, have been performed on the data measured in this work as well as on data reported in literature.

1. Introduction

Studies of neutron induced reactions are of considerable significance, both for their importance to fundamental research in Nuclear Physics and Astrophysics and for practical applications. These tasks require improved nuclear data and high precision cross sections for neutron induced reactions. Furthermore, the formation of a high spin isomeric state in the residual nucleus of a reaction is of considerable importance for testing nuclear models, as it is governed by the spin distribution of the level densities and the level scheme of the nuclei involved [1–3]. The $^{191}\text{Ir}(n,2n)$ reaction presents an interesting case since the high spin value 11^- of the second isomeric state (m2) of ^{190}Ir relative to the corresponding value 4^- of the ground state (g), offers great sensitivity for such studies.

The $^{191}\text{Ir}(n,2n)^{190}\text{Ir}^{g+m1}$ reaction has been investigated in the past by many groups, including our group [4], from ~ 8 to ~ 24 MeV, with the data differing however, by as much as 20%. The differences in the case of $^{191}\text{Ir}(n,2n)^{190}\text{Ir}^{m2}$ reaction though, can reach up to 50% at some energies and in the high energy region there are only few data points in literature.

As for the $^{193}\text{Ir}(n,2n)$ reaction, there are many data sets in literature concentrated in the region of ~ 15 MeV, with many discrepancies among them, while only few data points exist in the lower and higher energy regions.

The purpose of the present work was to experimentally deduce the cross section of the $^{191}\text{Ir}(n,2n)^{190}\text{Ir}^{g+m1}$, $^{191}\text{Ir}(n,2n)^{190}\text{Ir}^{m2}$ and $^{193}\text{Ir}(n,2n)^{192}\text{Ir}$ reactions at $17.1 \pm$

0.3 and 20.9 ± 0.2 MeV, implementing the activation technique. Furthermore, theoretical statistical model calculations were performed using the code EMPIRE 3.2.2 and compared to all available experimental data.

2. Experimental procedure

2.1. Irradiations

The $^{191,193}\text{Ir}(n,2n)$ reaction cross sections have been measured at the 5.5 MV tandem T11/25 Accelerator Laboratory of NCSR “Demokritos”. The neutron beam was produced via the $^3\text{H}(d,n)^4\text{He}$ reaction. A new Ti-tritiated target of 373 GBq activity has been used, consisting of a 2.1 mg/cm² Ti-T layer on a 1 mm thick Cu backing. The flange with the tritium target assembly was air cooled during the deuteron irradiation. Two collimators of 5 and 6 mm in diameter were used and the deuteron beam current was measured both at the collimators and the target and was kept at $\sim 1 \mu\text{A}$. During the irradiations, the flux variation of the neutron beam was monitored by a BF₃ detector placed at a distance of 3 m from the neutron production. The spectra of the BF₃ monitor were stored at regular time intervals (~ 200 sec) in a separate ADC during the irradiation process. The absolute flux of the beam was obtained with respect to the cross section of the $^{27}\text{Al}(n,\alpha)$ reference reaction. A Au foil was also used to cross check the experimental neutron flux, as well as the simulated one, via the $^{197}\text{Au}(n,\gamma)$ reaction.

High purity Ir and Al natural samples of 1.3 cm in diameter, having a thickness of ~ 0.5 mm, were placed at a distance of ~ 2 cm from the tritium target and were

^a e-mail: vlastou@central.ntua.gr

irradiated for up to 96 h. The induced activity of product radionuclides was measured with two HPGe detectors of 56% and 100% relative efficiency, properly shielded with lead blocks to reduce the contribution of the natural radioactivity. The efficiency of the detectors at the position of the activity measurements (10 cm) was determined via a calibrated ^{152}Eu point source. Corrections for self-absorption of the sample, coincidence summing effects of cascading gamma rays and counting geometry were taken into account along with the decay of product nuclides over the whole time range, as well as the fluctuation of the neutron beam flux over the irradiation time.

2.2. Neutron beam characterization

A comprehensive understanding of the energy dependence of the neutron flux is of major importance for the reliability of neutron induced reaction cross section measurements. For the investigation of the quasi-monoenergetic neutron beams produced via the $^3\text{H}(d,n)$ reaction at the tandem Laboratory of NCSR “Demokritos”, the multiple foil activation method has been applied along with Monte Carlo simulations implementing the NeuSDesc and MCNP codes.

2.2.1. Monte Carlo simulations

In the absence of time-of-flight capabilities, the investigation of the neutron fluence energy dependence has been carried out using the Monte Carlo simulation codes NeuSDesc [5] and MCNP [6]. The NeuSDesc software (developed at IRMM) estimates the neutron energy distribution at any distance, taking into account the details of the tritiated target. The output can then be used as input for MCNP simulations in order to include all the other details of the experimental setup (Al flange, Cu backing, target foils etc). The results of the MCNP simulations for the neutron flux at 20.9 MeV, on the Al foil at the front of the multiple foil stack is shown in Fig. 1. The main origin of the long tail of parasitic neutrons arises from the Ti and Cu backing of the Tritium target, along with the Al flange, and is 2–3 orders of magnitude lower than the main neutron peak at 20.9 MeV. In the case of 17.1 MeV, the tail of parasitic neutrons is much lower.

2.2.2. Multiple foil activation

For the experimental investigation of the neutron beam flux, the multiple foil activation technique has been applied, which is widely used for the determination of the neutron flux density around the irradiated samples along with unfolding techniques [7–9]. As a trial case of the facility, the deuterons were accelerated to 2.0 MeV and passed through two $5\ \mu\text{m}$ Mo foils in order to degrade their energy to 0.8 MeV, where the cross section of the $^3\text{H}(d,n)^4\text{He}$ reaction is high enough to produce a neutron beam at 15.3 MeV at a flux of the order of $\sim 10^6\ \text{n/s} \cdot \text{cm}^2$.

High purity foils of natural Au, Ti, Fe, Al, Nb, and Co were placed in close contact, at a distance of 1.7 cm from the neutron beam production and were irradiated for several hours. The neutron induced reactions on these foils, namely $^{58}\text{Ni}(n,p)^{58}\text{Co}$, $^{93}\text{Nb}(n,2n)^{92\text{m}}\text{Nb}$, $^{197}\text{Au}(n,\gamma)^{198}\text{Au}$, $^{56}\text{Fe}(n,p)^{56}\text{Mn}$, $^{59}\text{Co}(n,\alpha)^{56}\text{Mn}$, $^{115}\text{In}(n,n')^{115\text{m}}\text{In}$, $^{46}\text{Ti}(n,p)^{46\text{m}+g}\text{Sc}$, $^{47}\text{Ti}(n,p)^{47}\text{Sc}$, $^{48}\text{Ti}(n,p)^{48}\text{Sc}$, $^{64}\text{Zn}(n,p)^{64}\text{Cu}$ and $^{27}\text{Al}(n,\alpha)^{24}\text{Na}$, have different threshold

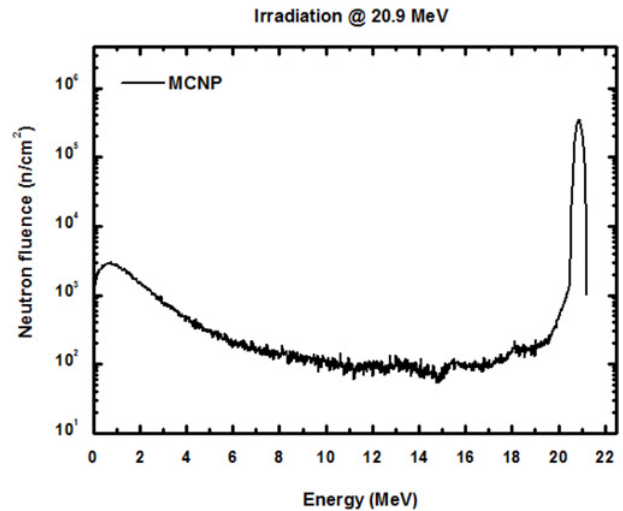


Figure 1. The simulated neutron energy distribution at 20.9 MeV, using the NeuSDesc and MCNP codes.

energies ranging from ~ 0 to ~ 9 MeV. The induced activities of product radionuclides were measured off-line by HPGe detector systems.

The experimental reaction rate R_i was deduced from the analysis of the experimental spectra for each of the above reactions i , according to the following expression:

$$R_i = \frac{\lambda_i N_i(t_B)}{N_{\tau i} [1 - \exp(-\lambda_i t_B)]}$$

with $N_i(t_B)$ being the number of residual nuclei, with decay probability λ_i , produced during the neutron activation time t_B and $N_{\tau i}$ the number of target nuclei for each reaction i .

In order to test the reliability of the simulations, the neutron spectral distribution of Fig. 1 has been used to calculate the simulated reaction rates ($R.R$) of the above reactions, using the expression:

$$R.R = \int_{E_{th,i}}^{\infty} \sigma_i(E) \cdot \Phi_i(E) dE$$

where $\sigma_i(E)$ are the excitation functions of the reactions taken from the ENDF/B-VII.1 library and $\Phi(E)$ the function of the neutron fluence normalized to the experimental fluence on each foil. In fact, the normalized neutron spectral distribution has been cut in energy slices ΔE starting from the threshold of each reaction up to the maximum neutron energy of 20.9 MeV and the sum

$$R.R = \sum_{\Delta E} \sigma(E) \cdot \Phi(E)$$

has been deduced. The resulting simulated reaction rates have been compared with the experimental ones and seem to agree well, thus verifying the reliability of the simulations.

3. Measurements and results

Natural Ir consists of two isotopes ^{191}Ir and ^{193}Ir having 37.3% and 62.7% abundances, respectively. Thus, the $^{193}\text{Ir}(n,2n)^{192}\text{Ir}$ threshold reaction is contaminated by the

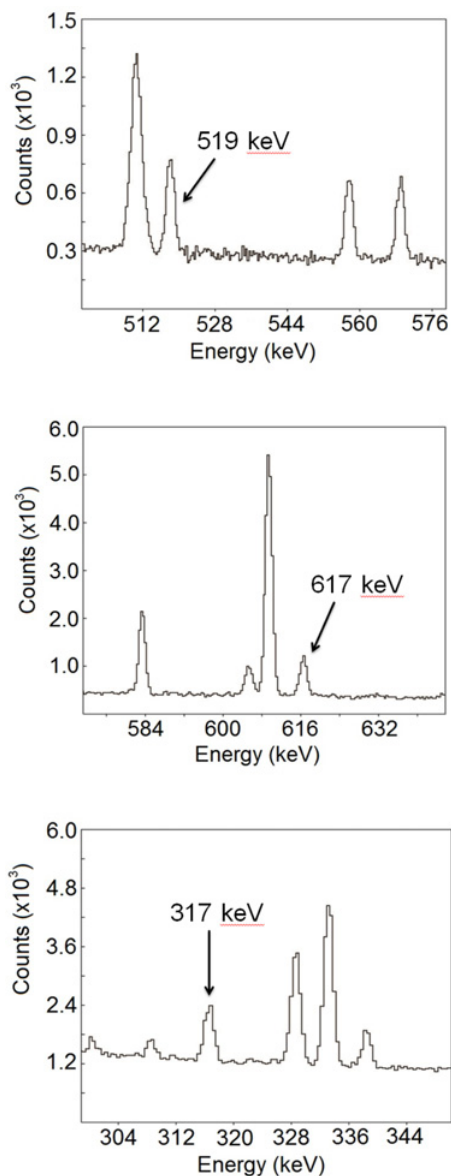


Figure 2. Experimental spectra from the decay of the g+m1 states (upper panel), m2 state (middle panel) of $^{191}\text{Ir}(n,2n)$ reaction and g+m1 states (bottom panel) of $^{193}\text{Ir}(n,2n)$ reaction after irradiation at 20.9 MeV. The acquisition time is 15 h for the middle panel and 50 h for the other two. The characteristic γ -rays used for the determination of the cross sections, are indicated with their energy values.

$^{191}\text{Ir}(n,\gamma)^{192}\text{Ir}$ reaction, which is affected by both high energy and mainly low energy parasitic neutrons. The experimental details for the appropriate corrections and the determination of (n,2n) reaction cross section for both Ir isotopes are described below.

3.1. The $^{191}\text{Ir}(n,2n)^{190}\text{Ir}$ reaction

The $^{191}\text{Ir}(n,2n)$ reaction leads to the formation of ^{190}Ir in its ground 4^- state ($T_{1/2} = 11.78$ d), as well as its metastable m1 1^- state ($T_{1/2} = 1.12$ h) and m2 11^- state ($T_{1/2} = 3.087$ h), which decay to ^{190}Os . Due to the short half life of m1, the sum of the metastable m1 and the ground state cross sections was determined via the most intensive 518.5 keV transition of ^{190}Os . The γ -spectroscopy measurements started 30 h at 17.1 MeV and

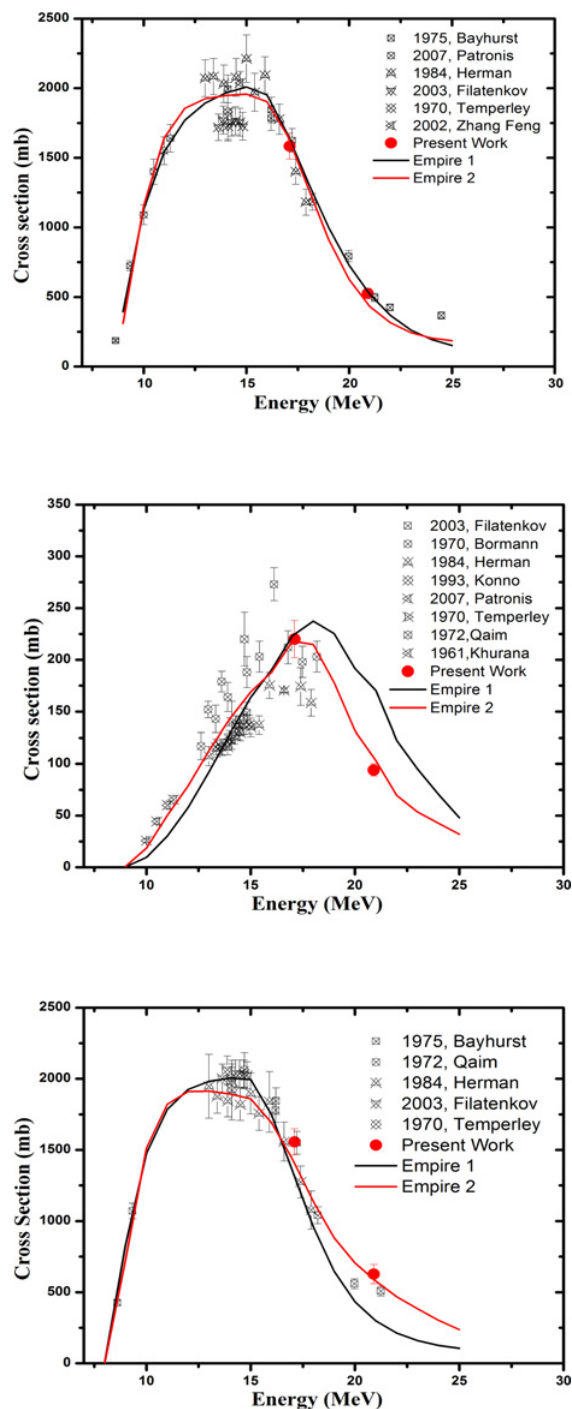


Figure 3. Experimental values of the present work at 17.1 and 20.9 MeV, along with EXFOR data from literature and theoretical calculations for the $^{191}\text{Ir}(n,2n)^{190}\text{Ir}^{g+m1}$ (upper part), $^{191}\text{Ir}(n,2n)^{190}\text{Ir}^{m2}$ (middle part) and $^{193}\text{Ir}(n,2n)^{192}\text{Ir}$ (lower part) reaction cross sections.

67 h at 20.9 MeV, after the end of the irradiation to ensure full decay of the m1 isomeric state to the ground state of ^{190}Ir and lasted for 50 h. The population of the second isomeric state m2 can be measured independently through the 616.5 keV transition of ^{190}Os [4], while the intensity measurements started 5 h at 17.1 MeV and 1 h at 20.9 MeV, after the end of the irradiation and lasted for 2 and 15 h, respectively. Figure 2 shows the γ -ray spectra emitted by the Ir sample after the irradiation at 20.9 MeV. The experimental cross sections for the population of the m2

and $g+m1$ states at 17.1 and 20.9 MeV are presented in Fig. 3 along with data from literature and theoretical predictions.

3.2. The $^{193}\text{Ir}(n,2n)^{192}\text{Ir}$ reaction

The residual nucleus ^{192}Ir decays to ^{192}Pt with a half life of 74.2 d. The characteristic γ -ray transitions 308.5, 316.5 and 468.1 keV from the de-excitation of ^{192}Pt can be used for the determination of the cross section of the $^{193}\text{Ir}(n,2n)^{192}\text{Ir}$ reaction. In this work, the most intensive one, namely the 316.5 keV (82.8%) has been used. The ^{192}Ir nucleus however, can also be produced by the $^{191}\text{Ir}(n,\gamma)$ reaction channel, which is always present and open to low energy parasitic neutrons. Thus, its contribution to the production of ^{192}Ir should be taken into account.

The contamination from the $^{191}\text{Ir}(n,\gamma)$ reaction has been deduced using the $\sigma(E)$ excitation function from the ENDF-VII library and the simulated $\Phi(E)$, normalized to the experimental fluence on the first Al foil, following the same procedure implemented in the multiple foil activation technique, as described in 2.2.2. The fine tuning of the low energy fluence (below 1 MeV), was accomplished through the normalization via the 411 keV γ -ray originating from the $^{197}\text{Au}(n,\gamma)$ reaction. This low energy part was subsequently used for the determination of the $^{191}\text{Ir}(n,\gamma)$ contribution to the yield of the 316.5 keV γ -ray. At 20.9 MeV this correction was of the order of 20%, while at 17.1 MeV the contamination was reduced to 2%. Naturally, this correction affects the overall uncertainty of the cross section for the $^{193}\text{Ir}(n,2n)$ reaction, shown in Fig. 3 along with data from literature and theoretical predictions.

4. Theoretical calculations

Theoretical calculations based on the compound nucleus theory of Hauser-Feshbach, were performed in the energy range 8–25 MeV using the code “EMPIRE” (3.2.2 version) [10], for both $^{191,193}\text{Ir}$ isotopes. Pre-equilibrium effects were taken into account via the multi-step direct (MSD) and multi-step compound (MSC)

formulations as implemented in the code. The sensitivity of the calculations for the reproduction of the cross section for both isotopes and mainly for the metastable state $m2$, was tested using several combinations of optical model potentials (OMP) for outgoing neutrons and nuclear level densities (NLD). The best results were achieved with the local OMP of M.B Chadwick [11] and Gilbert & Cameron NLD [12] (Empire 1) as well as with the spherical OMP of R.L. Varner [13] and the Generalized Superfluid Model (GSM, Ignatyuk et al) NLD [14] (Empire 2).

As for the outgoing protons, the EMPIRE specific OMP by Koning-Delaroche [15] was used. The results (Empire 1 and Empire 2) for the $(n,2n)$ reactions are shown in Fig. 3, while the existing data on (n,p) , $(n,3n)$ and (n,n') reactions on Ir, are also reproduced fairly well with the aforementioned parametrization.

References

- [1] P. Talou et al., Nucl. Sci. Eng. **155**, 84 (2007)
- [2] A. Fessler et al., Nucl. Sci. Eng. **134**, 171 (2000)
- [3] M. Avrigeanou et al., Phys. Rev. **C85**, 044618 (2012)
- [4] N. Patronis et al., Phys. Rev. **C75**, 034607 (2007)
- [5] E. Birgerssone and G. Lovestam, (2007) JRC Scientific and Technical Reports
- [6] J.F. Briesmeister, Ed., MCNP-a general Monte Carlo n-particle transport code. Report LA-13709 (2000)
- [7] R. Vlastou et al., Nucl. Instr. Meth. **B269**, 3266 (2011)
- [8] L. Olah et al., Nucl. Instr. Meth. **A404**, 373 (1998)
- [9] S.A. Jonath and K. Ibikunle, Nucl. Instr. Meth. **A501** (2003)
- [10] <http://www.nndc.bnl.gov/empire/>
- [11] R. Macklin and P.G. Young, Nucl. Sci. Eng. **97**, 239 (1987)
- [12] A. Gilbert and A.G.W. Cameron, Can. J. Phys. **43**, 1446 (1965)
- [13] R.L. Varner, et al., Phys. Rep. **201**, 57 (1991)
- [14] A.V. Ignatyuk et al., Sov. J. Nucl. Phys. **21**, 255 (1975)
- [15] A.J. Koning and J.P. Delaroche, Nucl. Phys. **A713**, 231 (2003)